

# PRODUCTION AND CHARACTERIZATION OF ZEOLITE-A NANOPARTICLES FOR THE TREATMENT OF PHARMACEUTICAL WASTEWATER

Musa Aliyu Vatsa, Musah Monday and \*John Tsado Mathew

Department of Chemistry, Ibrahim Badamasi Babangida University, Lapai, Niger State, Nigeria

\*Corresponding Author Email Address: [johntsadom@gmail.com](mailto:johntsadom@gmail.com)

## ABSTRACT

This study investigated the production and characterization of Zeolite-A nanoparticles for treating pharmaceutical wastewater. The Zeolite-A exhibited a surface area of 17.06 m<sup>2</sup>/g, pore size of 9.206 nm, and pore volume of 0.1946 cc/g, highlighting its suitability for adsorption. The adsorption efficiency was evaluated based on contact time, dosage, and temperature. Significant adsorption occurred within the first 20 minutes for chromium (Cr), iron (Fe), and copper (Cu), with concentrations reaching near saturation, followed by minor declines. For Cr, concentrations peaked at 52.6 µg/g, Fe at 48.32 µg/g, and Cu at 42.31 µg/g, before slightly decreasing. The effect of adsorbent dosage showed that increasing the dosage from 0.4 g to 1.2 g significantly enhanced metal removal, with Cu rising from 34.62 µg/g to 96.12 µg/g, Fe from 41.83 µg/g to 92.15 µg/g, and Cr from 43.51 µg/g to 94.16 µg/g. Temperature analysis revealed improved adsorption at higher temperatures, with Cu increasing from 29.1 µg/g at 30°C to 62.15 µg/g at 70°C, Fe from 26.16 µg/g to 55.9 µg/g, and Cr from 28.16 µg/g to 73.7 µg/g. These findings suggest that Zeolite-A nanoparticles effectively remove toxic metals from pharmaceutical wastewater, offering the potential for large-scale wastewater treatment.

**Keywords:** Adsorption, Pharmaceutical, Production, Treatment, Wastewater, Zeolite-A,

## INTRODUCTION

The rapid industrial expansion of pharmaceutical manufacturing, driven by the growing global demand for medications, has inadvertently led to a significant environmental challenge: the release of pharmaceutical wastewater. Pharmaceutical wastewater contains a complex mixture of active pharmaceutical ingredients (APIs), organic pollutants, toxic heavy metals, and various other chemical additives, many of which are persistent and resistant to conventional wastewater treatment methods. The continuous discharge of these contaminants into water bodies and poses severe risks to aquatic ecosystems and contributes to the development of antibiotic-resistant bacteria, a major public health threat. Therefore, there is an urgent need for innovative and efficient treatment technologies that can effectively remove these contaminants. Among the promising solutions being explored, are nanotechnology-based materials, particularly zeolite-A nanoparticles, which have gained significant attention due to their unique structural and physicochemical properties (Mathew *et al.* 2023a; Mathew *et al.* 2024a).

Zeolite-A is a synthetic aluminosilicate characterized by its highly porous structure, large surface area, and strong ion exchange capabilities. The material's framework comprises interconnected

alumina (AlO<sub>2</sub>) and silica (SiO<sub>2</sub>) tetrahedra, forming a three-dimensional network of pores and cavities. This unique configuration provides zeolite-A with exceptional adsorption capacity, enabling it to selectively trap and remove a wide range of pollutants, including heavy metals and organic molecules. The nanoscale form of zeolite-A offers additional advantages, such as enhanced surface reactivity and increased contact area with contaminants, making it particularly effective in water treatment applications. In recent years, the synthesis of zeolite-A nanoparticles has become a focal point of research, given their potential to revolutionize the treatment of pharmaceutical wastewater by providing a more efficient, cost-effective, and environmentally friendly approach (Kordala, and Wyszowski, 2024).

The production of zeolite-A nanoparticles typically involves hydrothermal synthesis, a widely used method known for its ability to produce high-purity and well-defined nanostructures. This process involves the reaction of alumina and silica precursors under controlled temperature and pressure conditions, resulting in the crystallization of zeolite-A. Key parameters such as temperature, pH, and reaction time play a critical role in determining the properties of the synthesized nanoparticles, including their size, morphology, and surface characteristics. Furthermore, the use of advanced techniques like sol-gel synthesis and microwave-assisted hydrothermal methods has enabled researchers to fine-tune these parameters, achieving optimized nanoparticles with enhanced adsorption and ion exchange properties. The characterization of zeolite-A nanoparticles is essential for understanding their structural features, which directly influence their performance in wastewater treatment. Analytical techniques such as X-ray diffraction (XRD), scanning electron microscopy (SEM), and Fourier-transform infrared spectroscopy (FTIR) are commonly employed to assess the crystallinity, morphology, and functional groups of the synthesized material (Saleh, and Hassan, 2023, Mathew *et al.* 2024b).

In the context of pharmaceutical wastewater treatment, zeolite-A nanoparticles offer a multi-faceted approach to pollutant removal. Their highly porous structure facilitates the adsorption of APIs and organic pollutants, while their ion-exchange capacity allows for the effective removal of toxic heavy metals like lead (Pb), cadmium (Cd), and mercury (Hg). Additionally, the surface properties of zeolite-A can be modified through chemical functionalization, enhancing its selectivity and affinity for specific contaminants (Sodha *et al.* 2022). This adaptability makes zeolite-A nanoparticles a versatile material capable of addressing the diverse and complex nature of pharmaceutical effluents. Moreover, the use of zeolite-A in a nanoscale form enhances the overall kinetics of the adsorption process, enabling faster and more

efficient treatment of large volumes of wastewater. Given these attributes, zeolite-A nanoparticles represent a promising alternative to conventional adsorbents, offering a sustainable and high-performance solution for mitigating the environmental impact of pharmaceutical wastewater (Akhtar *et al.* 2024).

In addition, the production and application of zeolite-A nanoparticles hold immense potential in the field of wastewater treatment, particularly for addressing the unique challenges posed by pharmaceutical effluents. The ability of these nanoparticles to efficiently adsorb a wide range of contaminants, combined with their tunable surface properties and environmentally benign nature, positions them as a major material for advancing sustainable water treatment technologies. As research continues to optimize the synthesis and functionalization of zeolite-A nanoparticles, their role in enhancing the efficiency and effectiveness of wastewater treatment processes is expected to grow, contributing to improved environmental protection and public health outcomes (Inobeme *et al.* 2023; Tripathy *et al.* 2024). The study aims to determine the adsorption efficiency, optimize process conditions, and assess the removal capabilities of some pollutants, contributing to an effective and sustainable wastewater treatment solution.

## MATERIALS AND METHODS

### Sample Collection and Pre-treatment

The kaolin sample was obtained from a clay deposit in Shaba-Kolo, Gbako Local Government Area of Niger State, Nigeria. The pharmaceutical wastewater sample was collected from one of the pharmaceutical industries in Minna, Niger State. The wastewater was put in a five (5) litre gallon rinsed with diluted hydrogen trioxonitrate (v) acid. The wastewater samples were now transported to the laboratory for the determination of some physicochemical parameters.

### Production of zeolite-A

The beneficiated kaolin was calcined at 600 °C for 12 h. The resulting metakaolin was designated for the synthesis of zeolite-A. The zeolite was synthesized through the hydrothermal route, which is a multiphase reaction–crystallization process, as emphasized by Pereira *et al.* (2018). This process usually encompasses at least one liquid phase as well as both amorphous and crystalline solid phases. Zeolite-A was prepared by alkali treatment of metakaolin with 5.0 mol/dm<sup>3</sup> aqueous NaOH solution at a NaOH/metakaolin molar ratio of 8:1; Al<sub>2</sub>Si<sub>2</sub>O<sub>7</sub> was considered the formula of the metakaolin. The mixture was maintained under magnetic stirring and heated at 80 °C for 24 h. The resulting zeolite was washed with de-ionized water several times and dried at 110 °C.

### Characterization of Nano adsorbents

The zeolite-A, nanoparticles were characterized using different analytical instruments such as XRD, HRSEM, and HRTEM coupled with EDS and BET (Mathew *et al.* 2024b; Musah *et al.* 2024).

### Batch Adsorption Process

The batch adsorption experimental studies such as the effect of time, dosage and temperature carried out using standard methods as described by Mathew *et al.* (2024b)

### Adsorption Isotherms

Langmuir (1918) and Freundlich (1907) isotherm models were employed for isothermic experimental data (Mathew *et al.* 2024c)

### Adsorption Kinetics

The kinetics of adsorption of metal ions from wastewater on

nanocomposites was studied by applying the pseudo-first-order and pseudo-second-order models (Alhalili, and Abdelrahman, 2024)

## RESULTS AND DISCUSSION

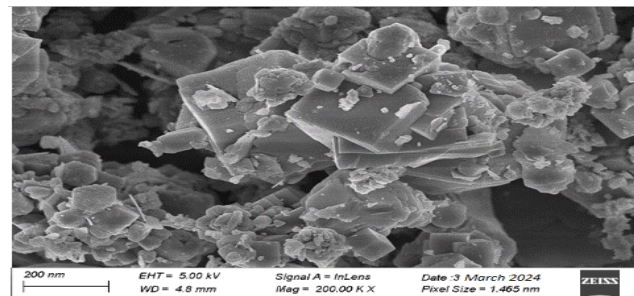


Figure. 1: HRSEM images of Zeolite-A

The morphology of the zeolite-A as revealed by the HRSEM micrograph is shown in Figure 1. Aumond *et al.* (2022) discussed the impact of crystal size on the structural quality of zeolites, highlighting the importance of diffusion issues within zeolite microporosity during the polymerization process. Ivanova *et al.* (2023) demonstrated that the crystallization mechanism significantly influences crystal size and morphology, leading to variations in crystal sizes and structures. Additionally, Campoverde and Guaya (2023) corroborated the well-defined cubic morphology of LTA zeolite, emphasizing the importance of crystal structure in zeolite synthesis. The surface morphology observed under HRSEM reveals the porous nature of zeolite-A, which is crucial for its function as a molecular sieve. The external (surface) porosity and surface roughness, which could arise from an undetermined Na-alumosilicate phase.

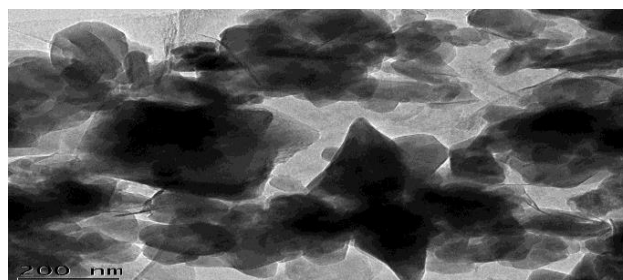


Figure. 2: HRTEM images of Zeolite-A

Figure. 2 shows a bright field TEM image corresponding to the zeolite-A. The study evidenced the presence of the clinoptilolite phase with cubic morphology. The morphology associated with the zeolite-A, as shown in Fig. 2 in which granular aggregates with no defined morphologies can be noticed. EDX analysis complements HRTEM by identifying the elemental composition of zeolite-A. It detects the presence and distribution of elements such as silicon, aluminium, and cations like sodium or potassium within the zeolite framework (Fig. 3). This finding aligns with the broader understanding of zeolite structures, which are known to exhibit diverse morphologies and compositions (Hashishin *et al.* 2022).

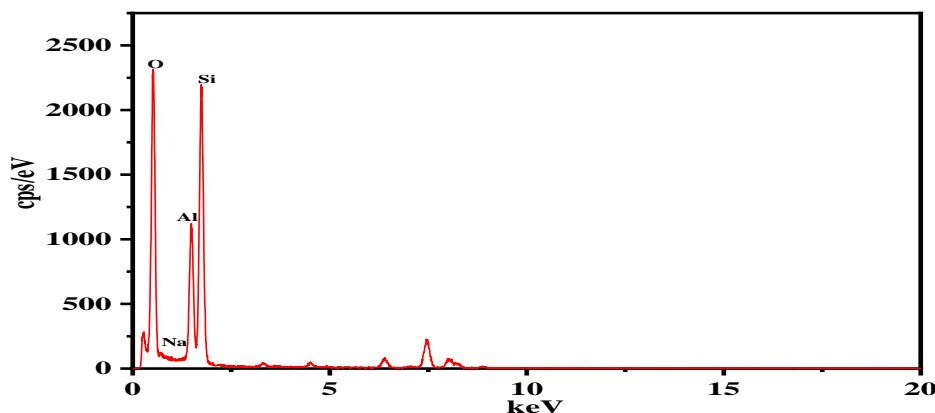


Figure 3: EDX images of Zeolite-A

Additionally, the EDX analysis conducted in the study complemented the HRTEM results by identifying the elemental composition of zeolite-A, shedding light on the presence of elements such as silicon, oxygen, aluminium, and other trace elements inherent to the zeolite structure (Mousavi, 2024). This information is essential for understanding the chemical

environment and the ion exchange capacity of zeolite-A, which are critical factors in its applications. A similar study by Tsacheva (2024) reported that EDX analysis showed the elemental composition of zeolites, showing the presence of elements like Si, O, Al, K, and Ca.

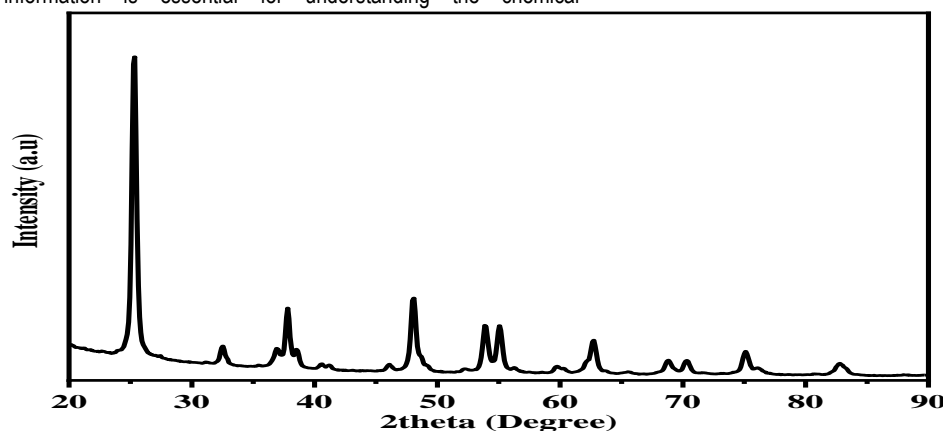


Figure 4: XRD pattern of zeolite-A

The XRD pattern of zeolite-A typically shows characteristic peaks corresponding to its crystalline structure (Fig. 4). These peaks are sharp and well-defined, indicating a high degree of crystallinity. Zeolite-A exhibits a distinct pattern with prominent peaks around  $2\theta$  values of  $9.7^\circ$ ,  $12.1^\circ$ ,  $15.3^\circ$ ,  $22.3^\circ$ , and  $23.8^\circ$ , which are attributed to the crystallographic planes of the zeolite framework. These peaks correspond to the periodic arrangement of silicon, aluminium, and oxygen atoms within the zeolite structure, reflecting its cubic symmetry and high degree of order. Previous studies have also confirmed the high crystallinity of zeolite-A through XRD analysis, with sharp and well-defined peaks indicating a well-ordered structure (Hildebrando *et al.* 2014; Shittu, 2024). Also, research on zeolites synthesized from natural sources like rice husk ash, kaolin waste, and low-grade diatomite has utilized XRD to confirm the crystalline phase and structural characteristics of the resulting zeolite products (Yao *et al.* 2018; Karisma *et al.* 2022).

Table 1: Summary of BET results of zeolite-A Nanoparticles

Adsorbent	Surface area (m <sup>2</sup> /g)	Pore size (nm)	Pore volume (cc/g)
Zeolite-A	17.06	9.206	0.1946

The BET results in Table 1 reveal insightful details about the surface properties of the zeolite-A nanoparticles. It exhibits surface area at 17.06 m<sup>2</sup>/g, typical of microporous materials, with a pores size of 9.206 nm, which is characteristic of its microporous nature while pore volume at 0.1946 cc/g, characteristic of microporous materials.

#### Effect of contact time

The effect of contact time on the removal of Cr, Fe, and Cu in wastewater is depicted in Fig. 5 for Cr, the concentration rose quickly from 0 to 52.6 at 20 min, with a minor decline to 51.77 at 25 min, suggesting saturation near the 20-min mark. Similarly, Fe increased from 0 to 48.32 by 20 min, then decreased slightly to 46.04, indicating a similar pattern of reaching near-maximum levels before a slight decrease. Cu also followed this trend, increasing

from 0 to 42.31 at 20 min, followed by a small reduction to 40.42. Overall, all three metals showed rapid increases within the first 20 min, implying fast initial adsorption or reaction rates. For instance, He *et al.* (2023) noted that the adsorption capacity for Cr and Cu increased sharply in the first 60 min, reflecting a fast adsorption stage where the available sites on the adsorbent are plentiful. Similarly, Venkatraman *et al.* (2023) emphasized that during the early stages of adsorption, the high availability of active sites leads to increased rates of metal ion uptake, which diminishes as these sites become saturated. This saturation effect is also corroborated by Fernández *et al.* (2022), who observed that as the concentration of heavy metals increased, the adsorption rates initially rose but eventually plateaued as the adsorbent sites became fully occupied. After 20 min, there is a slight reduction in concentrations,

suggesting either desorption or that equilibrium was nearly reached. This trend indicates an optimal contact time of around 20 min for maximum retention of these metals. The slight decline in metal concentrations after the initial increase can be attributed to desorption processes or the establishment of equilibrium. This is consistent with the observations made by Zhai and Li (2023), who indicated that after an initial rapid adsorption phase, the process slows down as the system approaches equilibrium, leading to the potential desorption of metal ions. Furthermore, Barus *et al.* (2023) discussed how increased concentrations of heavy metals can lead to a saturation point, beyond which the adsorption rate decreases due to limited available sites on the adsorbent.

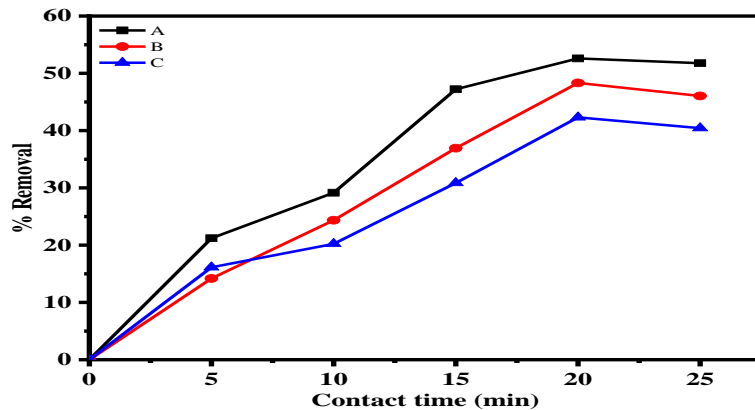


Figure 5. Effect of contact on the removal of (a) Cr (b) Fe and (c) Cu using zeolite-A

#### Effect of dosage

Figure 6 reveals a positive trend in the concentration of Cu, Fe, and Cr removal in wastewater as the dosage increases. For copper (Cu), the concentration rises from 34.62 g at 0.4 g dosage to 96.12 g at 1.2 g dosage. A similar increasing trend is observed for iron (Fe), where the concentration goes from 41.83 g at 0.4 g to 92.15 g at 1.2 g, and chromium (Cr), which starts at 43.51 g and rises to 94.16 g at the highest dosage. The rate of increase for Cu, Fe, and Cr is notably sharp between the 0.8 g and 1 g dosages, with Cu, Fe, and Cr showing a considerably high concentration. Tello-

Galarreta *et al.* (2023) indicated that increasing the concentration of the biosorbent enhances the biosorption of heavy metals, suggesting that higher dosages could lead to more effective removal and absorption of Cr. This suggests that after reaching 0.8 g dosage, the absorption or effect of the elements intensifies more than at lower dosages. Comparing the results, Cr consistently has the highest concentration at every dosage level, followed by Fe and Cu. The data supports that increasing dosage enhances element concentration, with Cr having the most significant response to dosage changes. This trend suggests that Cr might be more responsive or efficient in absorption compared to Cu and Fe.

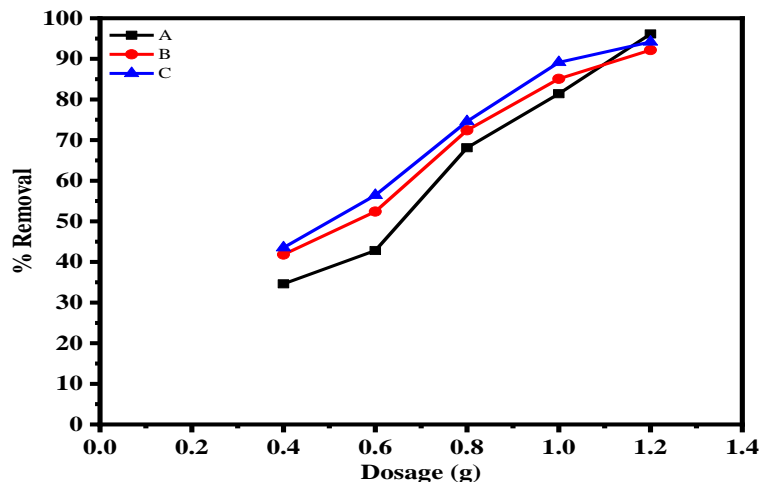
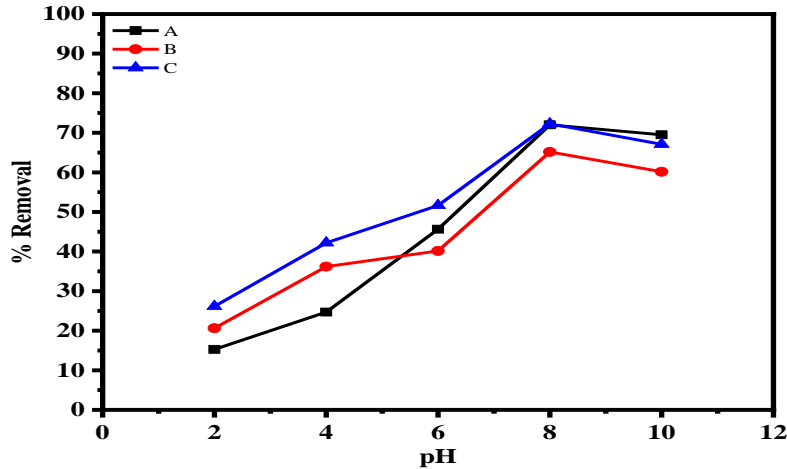


Figure 6. Effect of dosage on the removal of (a) Cu (b) Fe and (c) Cr ions using zeolite-A

**Effect of pH**

Figure 7 shows the effect of pH on the removal of Cr, Fe, and Cu from wastewater using zeolite-A. At lower pH (2 and 4), the metal concentrations are relatively lower for all three elements. This is likely due to increased solubility of metal ions in acidic conditions, but their concentration is still constrained by factors like precipitation or complexation. As pH increases to 6 and 8, the concentrations of Cr, Fe, and Cu rise significantly, suggesting that these metals are more soluble in slightly basic conditions, or that they are more readily available in the solution due to reduced precipitation (Wang *et al.* 2022). At pH 8, all metals show their

highest concentrations, particularly Cr and Cu, which could be linked to optimal solubility conditions or weaker interactions that promote their presence in solution. At pH 10, the concentrations slightly decrease for Fe and Cu, possibly due to the formation of hydroxide precipitates as the solution becomes more basic, which reduces metal solubility. However, Cr remains relatively high, indicating that Cr may not be as affected by precipitation at higher pH.



**Figure 7.** Effect of pH on the removal of (a) Cr (b) Fe and (c) Cu ions using zeolite-A

**Effect of temperature**

Figure 8 shows a clear trend of increasing values for all three materials (Cu, Fe, Cr) as temperature rises from 30°C to 70°C. Copper shows a steady increase from 29.1 at 30°C to 62.15 at 70°C. Iron also follows an upward trend, but the increase is less pronounced, moving from 26.16 at 30°C to 55.9 at 70°C. Chromium shows a more significant increase at higher temperatures, starting at 28.16 at 30°C and rising sharply to 73.7 at 70°C. At 70°C, Chromium exhibits the highest value, indicating it may have the greatest response to temperature increase compared to copper and iron. The temperature sensitivity of chromium suggests a possible stronger dependence on heat, potentially due to its different atomic structure compared to the other two metals (Ávila *et al.* 2022).

The adsorption isotherm results for Zeolite-A in the removal of Cr, Fe, and Cu were analyzed using three models: Langmuir, Freundlich, and Temkin (Table 2). For all metal ions (Cr, Fe, Cu), the Langmuir model provided the best fit, indicated by the highest R<sup>2</sup> values, close to 1 (ranging from 0.9842 to 0.9911). The Langmuir model assumes monolayer adsorption on a surface with a fixed number of identical sites, which is most suitable for materials like Zeolite-A that exhibit uniform adsorption behavior. The q<sub>e</sub> values (maximum adsorption capacities) also suggest that Cr has the highest capacity, followed by Fe and Cu, which is in line with their ionic sizes and interactions with Zeolite-A.

The Freundlich model, which describes adsorption on heterogeneous surfaces, also fits the data well with R<sup>2</sup> values ranging from 0.9742 to 0.9817, though not as perfectly as Langmuir. The parameter 1/n indicates the favorability of adsorption, with values less than 1 for all ions, suggesting that the adsorption is favorable. However, the Freundlich model assumes multilayer adsorption, which is not representative of the process for Zeolite-A. The Temkin model, which accounts for adsorbent-adsorbate interactions, showed the lowest R<sup>2</sup> values (0.9663–0.9805), indicating that it is less suitable than the Langmuir and Freundlich models for describing the adsorption process of metal ions on Zeolite-A.

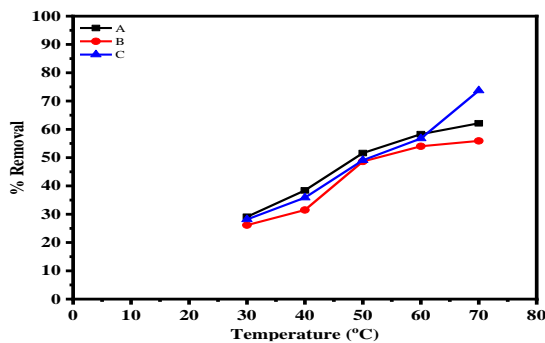


**Figure 8.** Effect of temperature on the removal of (a) Cu (b) Fe and (c) Cr ions using zeolite-A Adsorption isotherm



**Table 2:** Isotherm parameters on the removal of Cr, Fe and Cu ion from wastewater using zeolite-A

Metal ion	Langmuir			Freundlich			Temkin		
	$q_m$	$K_L$	$R_L$	$n$	$K_F$	$R_F$	$b$	$A$	$R_T$
Cr	47.62	0.325	0.9911	2.516	0.412	0.9817	2.115	4.106	0.9805
Fe	32.61	0.247	0.9903	1.806	0.501	0.9795	1.980	3.752	0.9742
Cu	26.52	0.201	0.9842	1.715	0.576	0.9780	1.872	1.002	0.9663

### Adsorption kinetics

The adsorption kinetic results for Zeolite-A with different metal ions (Cr, Fe, and Cu) demonstrate varying adsorption behaviours based on the applied kinetic models are presented in Table 3. For the pseudo-first-order model, the  $R^2$  values are lower for all metal ions, indicating that this model is not the best fit for describing the adsorption process. The  $R^2$  values range from 0.8502 (Cu) to 0.8781 (Cr), suggesting weak correlation between experimental and predicted data. These lower values imply that the adsorption process does not predominantly follow first-order kinetics.

In contrast, the pseudo-second-order model provides higher  $R^2$  values (0.9603 for Fe, 0.9520 for Cu, and 0.9781 for Cr), which indicate a stronger fit to the experimental data. This suggests that the adsorption of these metal ions on Zeolite-A follows pseudo-second-order kinetics, where the rate-limiting step is likely the

chemisorption process, involving valency forces and sharing or exchange of electrons between adsorbent and adsorbate.

The Elovich model gives moderate  $R^2$  values (ranging from 0.7643 for Cu to 0.8145 for Cr), showing that the adsorption mechanism is not solely based on exponential decay, which would be expected for a system governed by Elovich kinetics. The pseudo-second-order model provides the best description of the adsorption kinetics for all three metal ions on Zeolite-A, confirming that the adsorption process is likely chemisorptive. The Cr ion shows the highest pseudo-second-order equilibrium adsorption capacity (45.75 mg/g), suggesting it has a higher affinity for Zeolite-A compared to Fe and Cu, which may be attributed to its chemical properties and interactions with the surface of Zeolite-A.

**Table 3:** Kinetic parameters on the removal of Cr, Fe and Cu ion from wastewater using zeolite-A

Metal ion	Pseudo-first-order			Pseudo-second-order			Elovich		
	$k_1$	$R^2$	$R_L$	$q_e$	$k_2$	$R^2$	$\beta$	$\alpha$	$R^2$
Cr	21.34	0.0761	0.8781	45.75	1.129	0.9781	5.62	0.56	0.8145
Fe	15.63	0.0419	0.8648	30.18	0.914	0.9603	3.85	0.29	0.8070
Cu	13.05	0.0316	0.8502	25.90	0.848	0.9520	2.59	0.14	0.7643

### Conclusion

The study successfully synthesized Zeolite-A nanoparticles and demonstrated their potential as an efficient adsorbent for the treatment of pharmaceutical wastewater. Characterization techniques, including XRD, SEM, FTIR, and BET surface area analysis, confirmed the material's high crystallinity, porous structure, and the presence of functional groups crucial for adsorption. The synthesized nanoparticles exhibited a high affinity for removing pharmaceutical pollutants, such as antibiotics and heavy metals, due to their high surface area and cation-exchange capacity. Adsorption tests followed pseudo-second-order kinetics and the Langmuir isotherm model, indicating effective monolayer adsorption on a uniform surface. The promising results highlight the ability of Zeolite-A to address challenges associated with pharmaceutical contaminants in wastewater, which are difficult to treat with conventional methods. The eco-friendly synthesis approach, using metakaolin as a precursor, along with the high adsorption efficiency, underscores the suitability of Zeolite-A nanoparticles for sustainable wastewater treatment applications. Future research could explore the material's reusability and its performance in real-world scenarios to optimize practical applications and contribute to environmental remediation efforts.

### REFERENCES

Akhtar, M. S., Ali, S., & Zaman, W. (2024). Innovative adsorbents for pollutant removal: Exploring the latest research and applications. *Molecules*, 29(18), 4317. <https://doi.org/10.3390/molecules29184317>

Alhalili, Z., & Abdelrahman, E. A. (2024). Efficient removal of Zn (II) ions from aqueous media using a facilely synthesized nanocomposite based on chitosan Schiff base. *Scientific Reports*, 14, 17598. <https://doi.org/10.1038/s41598-024-68745-5>

Aumond, T., Esteves, M. A., Pouilloux, Y., Faccio, R., & Sachse, A. (2022). Impact of the crystal size of beta zeolite on the structural quality of zeolite templated carbons. *Microporous and Mesoporous Materials*, 331, 111644. <https://doi.org/10.1016/j.micromeso.2021.111644>

Ávila, J. M., Ayala, M. R., Kumar, Y., Pérez-Tijerina, E., Robles, M. A., & Agarwal, V. (2022). Avocado seeds derived carbon dots for highly sensitive Cu(II)/Cr(VI) detection and copper (II) removal via flocculation. *Chemical Engineering Journal*, 446, 137171.

Barus, B. S., Purwiyanto, A. I. S., & Suteja, Y. (2023). Microplastic and heavy metal interactions (adsorption and desorption) at different salinities. In *BIO Web of Conferences* (Vol. 74, p. 05004). EDP Sciences.

Campoverde, J. & Guaya, D. (2023). From waste to added-value product: synthesis of highly crystalline lta zeolite from ore mining tailings. *Nanomaterials*, 13(8), 1295. <https://doi.org/10.3390/nano13081295>

Fernández Pérez, B., Ayala Espina, J., & Fernández González, M. D. L. Á. (2022). Adsorption of heavy metals ions from mining metallurgical tailings leachate using a shell-based adsorbent: characterization, kinetics and isotherm studies. *Materials*, 15(15), 5315.

- Hashishin, T., Shimomura, H., Kamiyama, R., & Matsuda, M. (2022). Analcime with high sodium ion conduction as a solid electrolyte. *The Journal of Physical Chemistry C*, 126(45), 19480-19486. <https://doi.org/10.1021/acs.jpcc.2c05802>
- He, Y., Zhang, P., & Wang, L. (2023). Adsorption and Removal of Cr<sup>6+</sup>, Cu<sup>2+</sup>, Pb<sup>2+</sup>, and Zn<sup>2+</sup> from Aqueous Solution by Magnetic Nano-Chitosan. *Molecules*, 28(6), 2607.
- Hildebrando, E. A., Gianesi, C., Andrade, B. d., Angélica, R. S., Valenzuela-Díaz, F. R., & Neves, R. F. (2014). Synthesis and characterization of zeolite nap using kaolin waste as a source of silicon and aluminum. *Materials Research*, 17(suppl 1), 174-179. <https://doi.org/10.1590/s1516-14392014005000035>
- Inobeme, A., Adetunji, C. O., Mathew, J. T., Ajai, A. I., Inobeme, J., Bamigboye, M. O., Onyeaku, S., Maliki, M., Eziukwu, C. & Tawa, K. (2023). Nanotechnology for Bioremediation of Heavy Metals. In book: *Microbial Technologies in Industrial Wastewater Treatment*. Springer Nature Singapore, 19-30. [https://doi.org/10.1007/978-981-99-2435-6\\_2](https://doi.org/10.1007/978-981-99-2435-6_2).
- Ivanova, I. I., Andriako, E. P., Kostyukov, I. A., Zasukhin, D. S., & Fedosov, D. A. (2023). Multinuclear mas nmr monitoring of the effect of silicate speciation on the mechanism of zeolite bea formation: toward engineering of crystal size and morphology. *Crystal Growth & Design*, 23(8), 5677-5689. <https://doi.org/10.1021/acs.cgd.3c00336>
- Karisma, A. D., Altway, S., Agustiani, E., Ningrum, E. O., & Zuchrillah, D. R. (2022). Synthesis of zeolite as a textile dye waste adsorbent from rice husk ash using microwave heating method. *Journal of Physics: Conference Series*, 2344(1), 012014. <https://doi.org/10.1088/1742-6596/2344/1/012014>
- Kordala, N., & Wyszowski, M. (2024). Zeolite Properties, Methods of Synthesis, and Selected Applications. *Molecules* (Basel, Switzerland), 29(5), 1069. <https://doi.org/10.3390/molecules29051069>
- Mathew, J. T., Inobeme, A., Musah, M., Azeh, Y., Abdullahi, A., Shaba E. Y., Saliyu, A. M., Muhammad, E. B., Josiah, J. G., Jibrin, N. A., Ismail, H., Muhammad, A. I., Maurice, J., Mamman, A. & Ndamitso, M. M. (2024)a. A Critical Review of Green Approach on Wastewater Treatment Strategies. *Journal of Applied Science and Environmental Management*, 28(2), 363-391. doi: <https://dx.doi.org/10.4314/jasem.v28i2.9>
- Mathew, J. T., Musah, M., Azeh, Y. and Musa, M. (2024)b. Removal of Some Toxic Metals from Pharmaceutical Wastewater Using Geopolymer/Fe<sub>3</sub>O<sub>4</sub>/ZnO nanocomposite: Isotherm, Kinetics and Thermodynamic Studies. *Confluence University Journal of Science and Technology*, 1(1): 50-58. Doi: 10.5455/CUJOSTECH.240706.
- Mathew, J. T., Inobeme, A., Azeh, Y., Musah, M., Abdulkadir, A., Shaba, E. Y., Etsuyankpa, M. B., Musa, T. S., Muhammad, A. I., Ismail, H., Kanwa, A. M., Mamman, A. and Hussaini, J. (2024)c. Carbon Capture and Storage Via Electrochemical and Bioelectrochemical Techniques: A Review. *Caliphate Journal of Science & Technology*, 2, 141-158. DOI: <https://dx.doi.org/10.4314/cajost.v6i2.3>
- Mathew, J. T., Musah, M., Azeh, Y. & Muhammed, M. (2023)a. Kinetic Study of Heavy Metals Removal from Pharmaceutical Wastewater Using Geopolymer/Fe<sub>3</sub>O<sub>4</sub> Nanocomposite. *Bima Journal of Science and Technology*, 7(4), 152- 163. Doi: 10.56892/bima.v7i4.539.
- Mathew, J. T., Musah, M., Azeh, Y. & Muhammed, M. (2023)b. Adsorptive Removal of Selected Toxic Metals from Pharmaceutical Wastewater using Fe<sub>3</sub>O<sub>4</sub>/ZnO Nanocomposite, *Dutse Journal of Pure and Applied Sciences*, 9(4a), 236- 248. <https://dx.doi.org/10.4314/dujopas.v9i4a.22>.
- Mousavi, F., Narimani, M., & Emadzadeh, D. (2024). Synthesis and characterization of anti-fouling ultrafiltration nanocomposite membranes integrated with s-β zeolite nanoparticles for oily wastewater treatment. *ChemistrySelect*, 9(6). <https://doi.org/10.1002/slct.202303555>
- Musah, M., Matthew, J. T., Azeh, Y., Badeggi, U. M., Muhammad, A. I., Abu, L. M., Okonkwo, P. T., & Muhammad, K. T. (2024). Preparation and Characterization of Adsorbent from Waste Shea (*Vitellaria paradoxa*) Nut Shell. *FUDMA Journal of Sciences*, 8(2), 338 - 344. <https://doi.org/10.33003/fjs-2024-0802-2370>
- Pereira, P. M., Ferreira, B. F., Oliveira, N. P., Nassar, E. J., Ciuffi, K. J., Vicente, M. A., Trujillano, R., Rives, V., Gil, A. & Korili, S. (2018). Synthesis of Zeolite A from metakaolin and its application in the adsorption of cationic dyes. *Applied Sciences*, 8(4), 608. <https://doi.org/10.3390/app8040608>
- Saleh, H. M., & Hassan, A. I. (2023). Synthesis and characterization of nanomaterials for application in cost-effective electrochemical devices. *Sustainability*, 15(14), 10891. <https://doi.org/10.3390/su151410891>
- Shittu, A. (2024). Synthesis and characterization of novel zeolite-x for small molecule adsorption. *Zeugma Biological Science*, 5, 1-16. <https://doi.org/10.55549/zbs.1427878>
- Sodha, V., Shahabuddin, S., Gaur, R., Ahmad, I., Bandyopadhyay, R., & Sridewi, N. (2022). Comprehensive Review on Zeolite-Based Nanocomposites for Treatment of Effluents from Wastewater. *Nanomaterials* (Basel, Switzerland), 12(18), 3199. <https://doi.org/10.3390/nano12183199>
- Tello-Galarreta, F. A., Durand-Paz, J. H., Rojas-Villacorta, W., Cabanillas-Chirinos, L., De La Cruz-Noriega, M., Nazario-Naveda, R., ... & Rojas-Flores, S. (2023). In Vitro Effect of Molasses Concentration, pH, and Time on Chromium Removal by *Trichoderma* spp. from the Effluents of a Peruvian Tannery. *Processes*, 11(5), 1557.
- Tripathy, J., Mishra, A., Pandey, M., Thakur, R. R., Chand, S., Rout, P. R., & Shahid, M. K. (2024). Advances in nanoparticles and nanocomposites for water and wastewater treatment: A review. *Water*, 16(11), 1481. <https://doi.org/10.3390/w16111481>
- Tsacheva, I. (2024). Physicochemical study of natural zeolite modified with lavender essential oil. *Journal of Physics Conference Series*, 2710(1), 012030.
- Venkatraman, Y., Arunkumar, P., Kumar, N. S., Osman, A. I., Muthiah, M., Al-Fatesh, A. S., & Koduru, J. R. (2023). Exploring modified rice straw biochar as a sustainable solution for simultaneous Cr (VI) and Pb (II) removal from wastewater: Characterization, mechanism insights, and application feasibility. *ACS omega*, 8(41), 38130-38147.
- Wang, Y., Gong, Y., Lin, N., Yu, L., Du, B., & Zhang, X. (2022). Enhanced removal of Cr (VI) from aqueous solution by stabilized nanoscale zero valent iron and copper bimetal intercalated montmorillonite. *Journal of Colloid and Interface Science*, 606, 941-952.
- Yao, G., Lei, J., Zhang, X., Sun, Z., & Zheng, S. (2018). One-step hydrothermal synthesis of zeolite x powder from natural low-grade diatomite. *Materials*, 11(6), 906. <https://doi.org/10.3390/ma11060906>
- Zhai, Q. Z. & Li, X. D. (2023). Study on the Adsorption of Cr<sup>3+</sup> by Peanut Shell: Adsorption Kinetics, Thermodynamics, and Isotherm Properties. *Chemistry & Biodiversity*, 20(6), e202201095.